# The Initial Conditions to Star Formation: Low-Mass Star Formation at Low Metallicity

Martino Romaniello

*European Southern Observatory*
*Karl-Schwarzschild-Strasse 2*
*D-85748 Garching b. Muenchen, Germany*

We summarize the current status and future developments of an on-going effort to identify and characterize the properties of low-mass ($\sim 1\ M_{\odot}$) pre-Main Sequence stars with sub-solar metallicity ($\sim Z_{\odot}/3$). The selection criteria of the sample are presented, together with selected properties of the candidate pre-Main Sequence stars: • the spatial distribution, which is conclusively less clustered than that of the high mass stars of the same young generation; • the accretion rate onto the central star, which is found to be significantly higher than in the Galaxy; • and the Initial Mass Function, with a logarithmic slope $\Gamma \gtrsim -1.7$. The systematic uncertainties on this latter quantity are thoroughly discussed.

*Keywords*: Stars: formation, Stars: mass function, Stars: pre-main sequence, Galaxies: Large Magellanic Cloud, Galaxies: stellar content

## 1 Introduction

The processes at play during star formation determine much of the appearance of the visible Universe. The shape of the stellar Initial Mass Function (IMF) and its normalization (the star-formation rate) are, together with stellar evolution theory, key ingredients in determining the chemical evolution of a galaxy and its stellar content. Yet, our theoretical understanding of the processes that lead from diffuse molecular clouds to stars is still very tentative, as many complex physical phenomena concur in producing the final results. While clear variations in the star-formation rate are observed in different regions of the Milky Way and in external galaxies, with their histories showing bursts and lulls (e.g., Tolstoy 2003), the observational evidence for (or against) variations in the IMF is often contradictory

From an observational standpoint, most of the effort to characterize and understand the process of star formation has traditionally been devoted to nearby Galactic star-forming regions,

such as the Taurus-Auriga complex, Orion, etc. If this, on the one hand, permits one to observe very faint objects at the best possible angular resolution, on the other it is achieved at the expense of probing only a very limited set of initial conditions for star formation (all these clouds have essentially solar metallicity, e.g., Padget 1996).

With a typical metallicity of about a third of the solar value (e.g., Hill et al 1995, Geha et al 1998, Cole et al 2000) the Large Magellanic Cloud (LMC) provides an ideal environment to study low-mass young stars:

- with a distance modulus of $18.57 \pm 0.05$ (see the discussion in Romaniello et al 2000), the LMC is our closest galactic companion after the Sagittarius dwarf galaxy. At this distance one arcminute corresponds to about 15 pc and, thus, one pointing with a typical imaging instrument comfortably covers almost any star forming region in the LMC (10 pc see, e.g., Hodge 1988);
- the depth of the LMC along the line of sight is negligible, at least in the central parts we consider (van der Marel & Cioni 2001). All of the stars can, then, effectively be considered at the same distance, thus eliminating a possible spurious scatter in the Color-Magnitude Diagrams;
- the extinction in its direction due to dust in our Galaxy is low, about $E(B-V) \simeq 0.05$ (Bessell 1991) and, hence, our view is not severely obstructed.

Studying the effects of a lower metallicity on star formation is also essential to understand the evolution of both our own Galaxy, in which a large fraction of stars were formed at metallicities below solar, and what is observed at high redshifts. As a matter of fact, the global star formation rate appears to have been much more vigorous at $z \simeq 1.5$ than it is today (Madau 1996 and subsequent incarnations of the so-called "Madau plot"). At that epoch the mean metallicity of the interstellar gas was similar to that of the LMC at present (e.g., Pei, Fall & Hauser 1999). This fact makes the study of star forming regions in the LMC especially important for the understanding of galaxy evolution.

Here we will concentrate on the detection and characterization of solar-type pre-Main Sequence (PMS) stars around SN 1987A in the LMC. We have chosen this particular field for several reasons: the occurrence of a type II supernova ensured the presence of a young generation of stars, the mild crowding, which allows for accurate photometry and, finally, the availability of superb data originally designed to study the Supernova itself.

## 2 Observations and data reduction

The field of SN 1987A in the LMC was repeatedly imaged over the years with the WFPC2 onboard the HST to monitor the evolution of its Supernova remnant. We have taken advantage of this wealth of data and selected from the HST archive a uniform dataset providing broad-band coverage from the ultraviolet to the near infrared, as well as imaging in the H$\alpha$ line. A description of the camera and its filter set can be found in Heyer et al (2004). All images are centered with the Planetary Camera chip on SN 1987A ($\alpha_{2000} = 05:35:28.26, \delta_{2000} = -69:16:13.0$), but have different position angles on the sky, resulting in complete coverage of an almost circular region of $130''$ (about 30 pc) in radius.

The data were processed through the standard Post Observation Data Processing System pipeline for bias removal and flat fielding. In all cases cosmic ray events were removed combining the available images after accurate registration and alignment.

The plate scale is 0.045 and 0.099 arcsec/pixel in the Planetary Camera and in the three Wide Field chips, respectively. We performed aperture photometry following the prescriptions

by Gilmozzi (1990) as refined by Romaniello (1998), *i.e.* measuring the flux in a circular aperture of 2 pixels radius and the sky background value in an annulus of internal radius 3 pixels and width 2 pixels. Due to the undersampling of the WFPC2 Point Spread Function, this prescription leads to a smaller dispersion in the Color-Magnitude Diagrams, *i.e.* better photometry, than PSF fitting for non-jittered observations of marginally crowded fields (Cool & King 1995, Romaniello 1998). Photometry for the saturated stars was recovered by either fitting the unsaturated wings of the PSF for stars with no saturation outside the central 2 pixel radius, or by following the method developed by Gilliland (1994) for the heavily saturated ones. The flux calibration was done using the internal calibration of the WFPC2 Whitmore (1995), which is typically accurate to within 5% at optical wavelengths. The spectrum of Vega is used to set the photometric zeropoints (VEGAMAG system).

### *2.1 From magnitudes and colors to luminosity and temperature*

Once the observed fluxes of the stars are carefully measured, we derive their intrinsic properties, *i.e.* luminosity and temperature, as well as the extinction caused by the intervening interstellar dust along the line of sight, using the prescriptions developed by Romaniello et al (2002). The intrinsic stellar parameters and their associated errors are derived with a minimum $\chi^2$ technique by comparing the observed magnitudes to the ones expected based on the theoretical stellar atmosphere models of Bessel et al (1998) computed in the HST-WFPC2 bands using the IRAF *synphot* task. In order to cope with the effects of interstellar dust we have used the the extinction law appropriate for this region of the LMC (Scuderi at al 1996). Let us stress here that, by convolving the theoretical spectra with the filter sensitivity curves provided in IRAF, we ensure that the observations are faithfully modeled. In particular, the red leak that affects the WFPC2 F336W ($U$-band-like) filter is properly taken into account.

The dereddening method is extensively described in Romaniello et al (2002), but let us briefly summarize it here:

1. stars for which both $E(B-V)$ and $T_{eff}$ can be simultaneously derived are selected according to their small photometric error and their location in the $Q_{UBI}$ vs $(U-I)$ plane. $Q_{UBI}$ is a reddening-free color defined as:

$$Q_{UBI} \equiv (U-B) - \frac{E(U-B)}{E(B-I)}\,(B-I)$$

   This color-based selection is aimed at solving the possible non-monotonicity of broad-band colors with temperature (see, for example, Allen 1973). The stars for which $E(B-V)$ and $T_{eff}$ can be derived simultaneously turn out to be hotter than 10,000 K or between 6,750 and 8,500 K.

   Also, a star's location in the $Q_{UBI}$ vs $(U-I)$ plane provides a first guess of its temperature and reddening;

2. for the stars selected in step 1, $E(B-V)$, $T_{eff}$, $L$ and their associated uncertainties are derived starting from the first guesses by performing a minimum $\chi^2$ multi-band fit of synthetic colors from Bessel (1998) to the observed magnitudes;

3. for each star for which $E(B-V)$ and $T_{eff}$ cannot be derived simultaneously because of its intrinsic temperature and/or too large errors, the reddening is set as the mean of the ones of its 4 closest neighbors with direct reddening determination. The corresponding rms is used as an estimate of the uncertainty on the adopted value of $E(B-V)$. The effective temperature, luminosity and associated errors are, then, derived from a minimum $\chi^2$ multi-band fit.

In the case of the field discussed here, there is, on average, one star with direct $E(B-V)$ determination every 13 arcsec$^2$. Of course, it is possible that a few stars have, in reality, extinction values significantly different from the local mean, but the global effect is negligible.

The errors on $E(B-V)$ and $T_{eff}$ are computed from the $\chi^2$ maps and propagated to the luminosity. A full discussion on the errors is reported in Romaniello et al (2002), but it is important to keep in mind here that the procedure outlined above does not introduce any systematic errors on the derived stellar parameters.

The resulting HR diagram for the field of SN 1987A is displayed in Figure 2, together with selected stellar isochrones. As it can be seen, the most luminous stars in the field have an age of about 12 Myrs.

## 3 Selection of candidate PMS stars

The task of identifying the candidate PMS stars is a particularly challenging one because they have the same optical broad-band properties as the much older population (1 Gyr of age and older) of stars of comparable mass ($1-2\ M_{\odot}$) that constitute the diffuse population in the LMC (cfr. the HR diagram in Figure 2). As a diagnostics of their PMS nature, then, we use two well-known features of Galactic Classical T Tauri stars, namely the H$\alpha$ and Balmer continuum excesses[a].

Both the Balmer continuum and H$\alpha$ emissions are thought to be linked to the accretion process from the circumstellar disk (e.g., Calvet et al 2002). As such, a correlation is to be expected between these two quantities. In Figure 1 we plot the excess Balmer emission versus the one in H$\alpha$: $m_{\rm F336W,obs}$ is the observed magnitude in the HST-WFPC2 F336W, *i.e.* $U$-band-like, filter $m_{\rm F336W,mod}$ is the corresponding photospheric one from the models of Bessel et al (1998), while the $(m_{\rm F675W}-m_{\rm F656N})$ color measures the H$\alpha$ equivalent width. Indeed, the correlation between $U$ and H$\alpha$ activity is apparent, providing a very important sanity check as to the pre-Main Sequence nature of these stars.

The location in the HR diagram of the stars with Balmer continuum excess is displayed in Figure 2 as black dots, overlaid on the general stellar population (grey squares).

Of course, this selection criterion based on H$\alpha$ and/or Balmer continuum excess does not provide a complete census of all of the PMS stars in the field. Rather, it privileges stars with high enough excesses to be detectable in our data. It would be highly desirable to use X-ray observations to select the PMS stars, a technique that has proven to be extremely successful in identifying low-mass PMS stars in Galactic star-forming regions. Regrettably, though, the current generation of X-ray instruments do not have enough sensitivity to reach as far out as the LMC.

## 4 The properties of candidate PMS stars in the LMC

### *4.1 The spatial ditribution*

In Figure 3 we display the spatial distribution of massive stars, *i.e.* stars with M>6 $M_{\odot}$, and candidate PMS stars as defined above through their H$\alpha$ excess ($M \lesssim 2\ M_{\odot}$). We see that massive stars are strongly concentrated near SN 1987A (14 out of a total of 55 are within 20″ of the supernova), and that 31 out of the remaining 41 are mostly located East of SN 1987A. The PMS stars, on the other hand, do not show any strong spatial concentration, although one

[a]Only stars with a measured H$\alpha$ equivalent width larger than 3 Å, or $(m_{\rm F675W}-m_{\rm F656N})>0.15$, are considered. Emission below this threshold could be contaminated by normal chromospheric activity (Frasca & Catalano 1994).

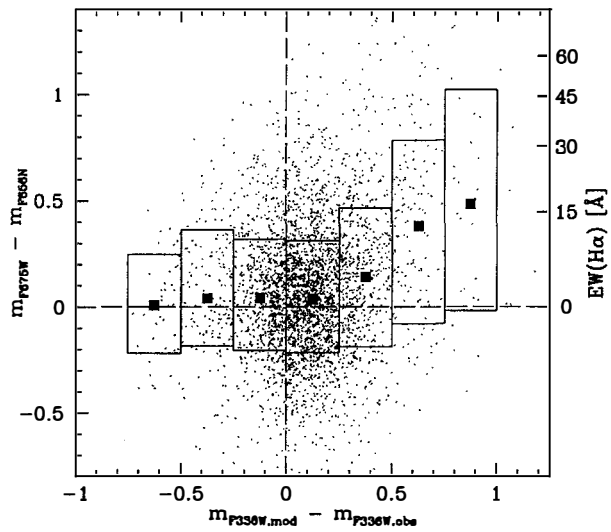


Figure 1: F336W vs Hα excess for our sample of candidate pre-Main Sequence stars in the field of SN 1987A (gray dots). $m_{F336W,obs}$ is the observed magnitude, $m_{F336W,mod}$ is the photospheric one from the models of Bessell et al (1998) and the $(m_{F675W} - m_{F656N})$ color measures the Hα equivalent width, as shown on the right vertical axis. The filled squares represent the median $(m_{F675W} - m_{F656N})$ value in the $(m_{F336W,mod} - m_{F336W,obs})$ bins marked by the rectangles, whose vertical extent includes 66% of the stars in each bin. The high statistical correlation between the two quantities is apparent and is confirmed by the high value of Spearman's coefficient $\rho = 7.9$, which implies a probability of less than $10^{-4}$ that the two variables are uncorrelated.

can notice that the number density of PMS stars on the NE side of SN 1987A is appreciably lower than on the SW side. It is apparent, then, that high and low-mass stars belonging to the same young generation are spatially distributed in substantially different manners, indicating that star formation processes for different ranges of stellar masses are rather different and/or require different initial conditions.

We do not find any significant difference in ages among PMS stars at different spatial locations, suggesting that, rather than dealing with some sort of propagating star formation, the key factor here is the overall efficiency of the star formation process that varies from place to place. Also, we note that there is no enhancement in the density of candidate PMS stars around the SN 1987A cluster, nor near the brightest star in the observed field lending support to the idea that the process of formation of low mass stars may be distinct from the one leading to the formation of massive stars.

### *4.2 The accretion rate*

There is currently a widespread agreement that low mass stars form by accretion of material until their final masses are reached (e.g., Bonnell et al 2001 and references therein). As a consequence, the accretion rate is arguably *the* single most important parameter governing the process of low-mass star formation and its final results, including the stellar Initial Mass Function. Ground and HST-based studies show that there may be significant differences between star formation processes in the LMC and in the Galaxy. For example, Lamers et al (1999) and de Wit et

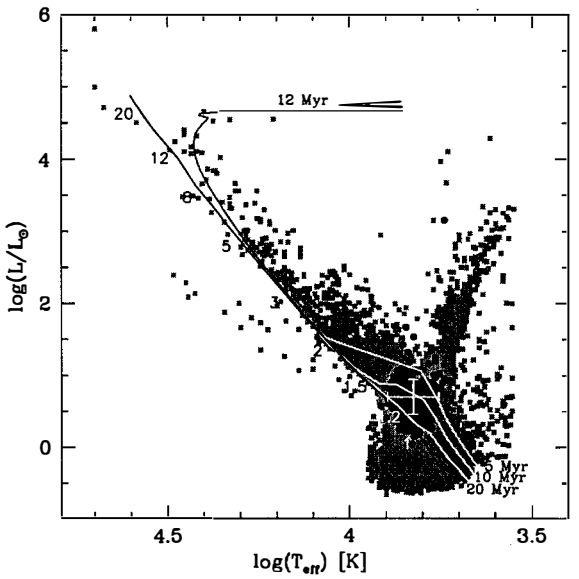


Figure 2: HR diagram displaying the position of the stars with $U$ excess (black dots) overlaid on the general stellar population (gray squares) found in the WFPC2 field. Luminosities and temperatures for the stars with excess were computed excluding the F336W magnitude from the fit to the model atmospheres and adopting for each star the mean $E(B-V)$ value of its 4 closet neighbors. The typical uncertainties on the luminosity and temperature for the stars with $U$ excess, computed as the mean of the uncertainties on the individual stars, is shown as a cross. For reference, we also plot the theoretical Zero Age Main Sequence, with the position of stars of various masses marked on it, and a 12 Myr post-Main Sequence isochrone ($Z = 0.3\ Z_{\odot}$, Brocato & Castellani 1993). Also shown are 5-20 Myrs pre-Main Sequence isochrones (Siess et al 1997), again computed for $Z = 0.3\ Z_{\odot}$.

al (2002) have identified by means of ground-based observations high-mass pre-Main Sequence stars (Herbig AeBe stars) with luminosities systematically higher than observed in our Galaxy, and located well above the "birthline" of Palla & Staler (1990). They attribute this finding either to a shorter accretion timescale in the LMC or to its smaller dust-to-gas ratio. Whether such differences in the physical conditions under which stars form will generally lead to differences at the low mass end is an open question, but Panagia et al (2000) offer tantalizing evidence of a higher accretion also for LMC low mass stars.

We have measured the accretion rate onto our solar-type candidate PMS star by means of their Balmer excess (Romaniello et al 2004). The idea that the strong excess emission observed in some Galactic low-mass, pre-Main Sequence stars (Classical T Tauri stars) is produced by accretion of material from a circumstellar disk dates back to the pioneering work of Lynden-Bell & Pringle (1974). The excess luminosity is, then, related to the mass accretion rate. In particular, the Balmer continuum radiation produced by the material from the disk as it hits the stellar surface has been used as an estimator of the mass infall activity (see, for example, Gullbring et al 1998 and references therein).

We have, then, derived the accretion rate onto the central star ($\dot{M}$) with the following equations:

$$\begin{cases} L_{acc} \simeq \frac{GM_*\dot{M}}{R_*}\left(1-\frac{R_*}{R_{in}}\right) \\ \log\left(\frac{L_{acc}}{L_\odot}\right) = 1.16\ \log\left(\frac{L_{\rm F336W,exc}}{L_\odot}\right) + 1.24 \end{cases} \quad (1)$$

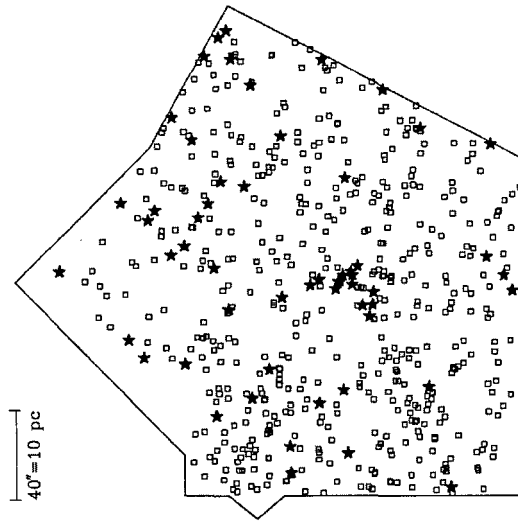


Figure 3: Comparison of the spatial distributions of massive stars ($M \gtrsim 6M_{\odot}$, filled star symbols) and PMS stars ($M \lesssim 2M_{\odot}$, open squares) belonging to the same younger population. North is up and East is to the left. As it can be seen, the stars of different mass have conclusively different spatial distributions.

The second equation is the Gullbring et al (1998) empirical relation between the accretion luminosity $L_{acc}$ and the Balmer excess luminosity, as transformed by Robberto et al (2004) to the WFPC2 F336W filter. The reader is referred to Romaniello et al (2004) for a thorough description of the derivation of $\dot{M}$.

When interpreted as pre-Main Sequence stars, the comparison of the objects' location in the HR diagram with theoretical evolutionary tracks (see Figure 2) allows one to derive their masses ($\sim 1 - 1.4\ M_{\odot}$) and ages ($\sim 12 - 16$ Myrs). At such an age and with an accretion rate as measured using equations (1) in excess of $\sim 1.5 \times 10^{-8} M_{\odot}\ yr^{-1}$, these candidate pre-Main Sequence stars in the field of SN 1987A are both older and more active than their Galactic counterparts known to date. In fact, the overwhelming majority of T Tauri stars in Galactic associations seem to dissipate their accretion disks before reaching an age of about 6 Myrs (Haisch et al 2001; Armitage et al 2003). Moreover, the oldest Classical T Tauri star know in the Galaxy, TW Hydræ, at an age of 10 Myrs, *i.e.* comparable to that of our sample stars, has a measured accretion rate some 30 times lower than the stars in the neighborhood of SN 1987A (Muzerolle et al 2000).

The situation is summarized in Figure 4, where we compare the position in the age-$\dot{M}$ plane of the stars described here with that of members of Galactic star-forming regions. An obvious selection bias that affects our census is that we only detect those stars with the largest Balmer continuum excesses, *i.e.* highest accretion rates. There might be stars in the field with smaller accretion rates, either intrinsically or because they were observed when the accretion activity was at a minimum, which fall below our detection threshold. This selection effect is rather hard to quantify, but it is clear that the locus of the accreting stars that we do detect in the neighborhood of SN 1987A is significantly displaced from the one defined by local pre-Main Sequence stars.

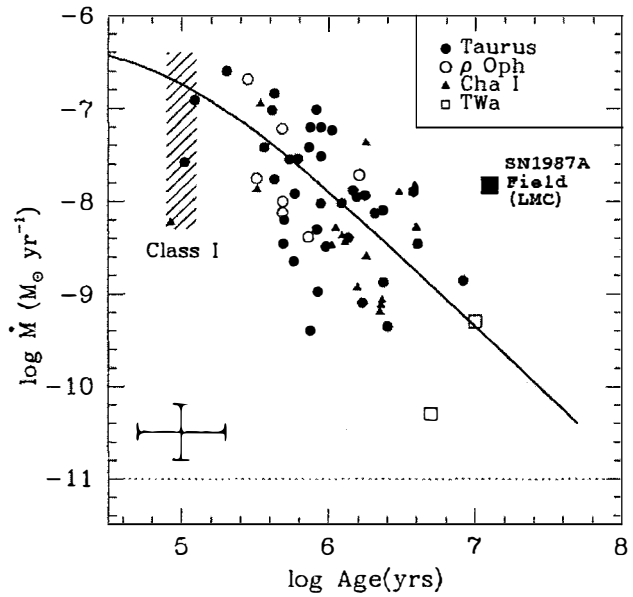


Figure 4: Mass accretion rate as a function of age for Classical T Tauri stars in different star-forming regions (adapted from Muzerolle et al 2000). Our result for the field of SN 1987A is marked with a black square.

### *4.3 The Initial Mass Function*

The almost anti-correlation of the spatial distributions of high mass and low mass stars of a coeval generation (cfr. Section 4.1 and Figure 3) indicates that star formation processes for different ranges of stellar masses are rather different and/or require different initial conditions. An important corollary of this result is that the very concept of an "initial mass function" may not have validity in detail, but rather be the result of a chaotic process. It would, then, only make sense to talk about an *average IMF* over a suitably large area in which all different star formation processes are concurrently operating. Actually, if we just take the ratio of the total numbers of massive to low-mass stars belonging to the young population as identified through their Balmer continuum excess, and interpret them in terms of a power-law IMF adopting mass intervals of 6-15 $M_{\odot}$ and 1-2 $M\odot$ for massive stars and for PMS stars, respectively, we would derive a slope of the initial mass function of $\Gamma = dlogN/dlogM \simeq -1.7$ with a purely statistical uncertainty of $\pm 0.1$. This value is somewhat steeper than the classical Salpeter's (1955) slope $\Gamma = -1.35$ for the Solar neighborhood and is valid over essentially the same mass interval as the original Salpeter's analysis, *i.e.* ~2-10 $M_{\odot}$. However, this is a conclusion drawn without taking into account of possible incompleteness effects.

On the one hand, for both massive and low mass stars above $\sim 1M_{\odot}$, incompleteness due to missed detection and/or to crowding/blending is a negligible effect because all of these stars are well above our detection limit and their surface density in not so high (1 star per $\sim$ 170 WF pixel area, or, equivalently, an average separation of stars of $\sim$ 13 WF pixels). On the other hand, for PMS stars one has bear in mind that we can reliably identify only stars with strong excess and that the *total* number of PMS stars of comparable masses may be considerably larger. For example, Alcalá et al (1996) have shown that in the Orion region the number of weak-line T Tauri stars, *i.e.* low-mass PMS stars that do not exhibit strong emission features, is at least

comparable to, and possibly larger than that of strong-line T Tauri stars.

Moreover, T Tauri stars are known to exhibit photometric variability on short timescales (e.g., Smith et al 1999, and references therein). As a consequence, at any one time one may be able to detect only a fraction of the entire population of strong-line T Tauri stars. Indeed, preliminary comparisons of overlapping regions in fields imaged at two different epochs (about 15% of the entire field around SN 1987A) have shown that, while the number of stars with a significant excess at any one time is essentially constant, no more than half of the candidate PMS stars display a significantly strong H$\alpha$ excess at both epochs (Romaniello et al, in preparation). This suggests that the "true" Initial Mass Function could significantly steeper than $\Gamma \simeq -1.7$ quoted above.

It is important to realize how crucial it is to *individually* identify and characterize each and everyone of the PMS stars if one wants to evaluate an IMF reliably, because using just the location of stars in the HR diagram as the criterion to recognize PMS stars will unavoidably introduce some heavy contamination from old stars in the process of leaving the Main Sequence. One can argue that, for a fixed surface density of old population stars, such an effect is much reduced when studying regions containing large concentrations of young stars. For instance, the possible contamination by older populations could be, say, 10% or less, if the surface density of young stars in a given region were higher than 200-400 times the density of young stars around SN 1987A or, equivalently, 10 times the density of old population stars in the SN 1987A vicinities. However, since the density of old population stars with luminosities in the range $1 < L/L_{\odot} < 10$ is about 0.2 stars per square arcsecond, exceeding that density by a factor of 10, at least, would imply an average density of young population, low mass stars ($1 < L/L_{\odot} < 10$) higher than 2 stars per square arcsecond, and at least ten times higher for stars in the next 1-*dex* bin in luminosity. It is easy to realize that with such high stellar densities another problem is bound to arise, at least for low mass stars, namely confusion/blending due to crowding. These effects will both "drown" faint stars into a "sea" of even fainter stars and/or would artificially create brighter stars by confusing nearby stars into one more luminous, apparently point-like source.

## 5 Future directions

From the discussions presented above, it is clear that it is essential to have *spectroscopic* criteria that allow one to discern PMS stars from field stars unambiguously and completely. H$\alpha$ and/or UV excess are possible ways of accomplishing this goal, but even these methods need confirmation, calibration and sharpening, in that we still have to compare our multi-band photometry with *real* spectra before a 100% reliable of identification of PMS stars can be claimed. In order to fill this gap we have just secured medium-resolution spectra of a number of our best PMS candidates at the ESO-VLT with the VIMOS instrument in IFU mode. The data reduction and analysis are currently in progress and should result in the first ever statistically significant sample of extragalactic low-mass pre-Main Sequence stars with a spectroscopic confirmation.

## References


1. Allen, C.W., 1973, Astrophysical Quantities (3rd ed.: London: Athlone)
2. Armitage, P.J., Clarke, C.J., and Palla, F. 2003, MNRAS, 342, 1139
3. Bessell, M.S. 1991, A&A, 242, L17
4. Bessell, M.S., Castelli, F., and Plez, B. 1998, A&A, 333, 231 (erratum 337, 321)
5. Bonnell, I.A., Clarke, C.J., Bate, M.R., and Pringle, J. E. 2001, MNRAS, 324, 573
6. Brocato, E., and Castellani, V. 1993, ApJ, 410, 99

7. Calvet, N., Hartmann, L., and Strom, S.E. 2002, in "Protostars and Planets IV", eds. V. Mannings, A.P. Boss, and S.S. Russell (Tucson: University of Arizona Press), 377
8. Cole, A.A., Smecker-Hane, T.A. and Gallagher, J.S., III 2000, AJ,120, 1808
9. Cool, A.M, and King, I.R. 1995, in "Calibrating HST: Post Servicing Mission", eds. A. Koratkar and C. Leitherer (Baltimore: STScI), 290
10. de Wit, W. J., Beaulieu, J. P., and Lamers, H.J.G.L.M. 2002, A&A, 395, 829
11. Frasca, A., and Catalano, S. 1994, A&A, 284,883
12. Geha, M.C., Holtzman, J.A., Mould, J.R., et al 1998, AJ, 115, 1045
13. Gilliland, R.L. 1994, ApJ, 435, L63
14. Gilmozzi, R. 1990, Core Aperture Photometry with the WFPC, STScI Instrum. Rep. WFPC-90-96 (Baltimore: STScI)
15. Gullbring, E., Hartmann, L., Briceño, C., and Calvet, N. 1998, ApJ, 492, 323
16. Haisch, K.E., Jr., Lada, E.A, and Lada, C.J. 2001, ApJ, 553, L153
17. Heyer, I., Biretta, J. et al. 2004, WFPC2 Instrument Handbook, Version 9.0 (Baltimore: STScI)
18. Hill, V., Andrievsky, S., and Spite, M. 1995, A&A, 293, 347
19. Hodge, P.W. 1988, PASP, 100, 1051
20. Lamers, H.J.G.L.M., Beaulieu, J. P., and de Wit, W. J. 1999, A&A, 341, 827
21. Lynden-Bell, D., and Pringle, J.E. 1974, MNRAS, 168, 603
22. Madau, P., Ferguson, H.C., Dickinson, M.E., et al 1996, MNRAS, 283, 1388
23. Muzerolle, J., Calvet, N., Briceño, C., Hartmann, L., and Hillenbrand, L. 2000, ApJ, 535, L47
24. Padgett, D.L. 1996, AJ, 471, 874
25. Palla, F., and Stahler, S. 1991, ApJ, 360, 47
26. Panagia, N., Romaniello, M., Scuderi, S., and Kirschner, R.P. 2000, ApJ, 539, 197
27. Pei, Y.C., Fall, S.M., and Hauser, M.G. 1999, ApJ, 522, 604
28. Romaniello, M. 1998, Ph.D. Thesis, Scuola Normale Superiore, Pisa
29. Romaniello, M., Salaris, M., Cassisi, S., and Panagia, N. 2000, APJ, 530, 738
30. Romaniello, M., Panagia, N., Scuderi, S., and Kirshner, R.P. 2002, AJ, 123, 91
31. Romaniello, M., Robberto, M., and Panagia, N. 2004, ApJ, 608, 220
32. Scuderi, S., Panagia, N., Gilmozzi, R., Challis, P.M., and Kirshner, R.P., 1996, ApJ, 465, 956
33. Siess, L., Forestini, M., and Dougados, C. 1997, A&A, 324, 556
34. Tolstoy, E. 2003, in "A decade of Hubble Space Telescope science", eds. M. Livio, K. Noll and M. Stiavelli, Space Telescope Science Institute symposium series, Vol. 14, Cambridge University Press, 128
35. van der Marel, R.P., and Cioni, M.-R.L. 2001, AJ, 122, 1807
36. Whitmore, B. 1995, in "Calibrating HST: Post Servicing Mission", eds. A. Koratkar and C. Leitherer (Baltimore: STScI), 269